MEOS GEO 2025

SPE-226924-MS

Modelling and attenuation of mode conversion noise: A case study of Egypt offshore

J. Kumar[1], M. Salem[1], M. Soliman[1], I. Ahmed[1], I. Diab[1], M. Raafat[1], J. Brittan[1]

[1]TGS

Introduction

In regions with significant salt presence, such as the Eastern Mediterranean, the pronounced contrast in acoustic velocity between salt bodies and surrounding sediments often leads to the generation of converted wave modes. These arise when compressional (P-wave) energy transforms into shear (S-wave) energy upon encountering the high-contrast boundaries at the top or base of the salt. As the converted waves travel at slower velocities, their arrival times differ from primary reflections and can appear as deeper, misleading signals in seismic records. This energy, if not properly managed, can hinder the accurate interpretation of subsurface structures.

One of the primary challenges in hydrocarbon exploration within the Messinian salt province of the Eastern Mediterranean is the contamination of P-wave images by such converted modes. The salt layer in this area typically exhibits interval velocities around 4200–4300 m/s, while the surrounding post- and pre-Messinian sediments display significantly lower velocities, ranging from 2400 to 3000 m/s. These sharp contrasts promote the generation of converted wave events, particularly at steeply dipping salt interfaces, and frequently lead to complex interference patterns in seismic images. Although some of these converted events can enhance illumination and provide additional insight into subsurface geometry, they more often act as noise that obscures true reflections, especially in sub-salt targets where accurate imaging is critical.

Among the various converted wave types, those converting at both the top and base of salt formations—such as PSPP and PPSP—pose a significant problem due to their higher amplitudes and complex moveout behavior. Symmetrical modes like PSSP, while theoretically present, often typically not observed in the field dataset due to weaker amplitude and longer travel times. Standard suppression techniques include filtering based on velocity discrimination or targeted muting via travel-time modeling, but these approaches may be ineffective in areas with irregular salt geometry.

To address this issue more robustly, we explore an alternative approach involving dual acoustic simulations. By running 3D acoustic modeling twice—once with the base salt interface included and once without—we isolate the energy associated with converted wave phenomena (Kumar et al., 2018). The resulting synthetic data enables a cleaner estimation of the converted wavefield, which can then be subtracted from the original gathers prior to migration. This method provides a more reliable suppression of mode-converted noise, especially in geologically complex regions.

This paper demonstrates the application of this modeling-based attenuation strategy on recently acquired multisensor datasets from the Eastern Mediterranean. The results highlight the potential of this approach to significantly improve image clarity, assist in amplitude-preserving workflows, and enhance the reliability of velocity model building in areas affected by strong P-S mode conversions.

Method

Converted mode contamination in P-wave seismic images remains a significant challenge in salt provinces, where sharp acoustic impedance contrasts at salt-sediment boundaries generate P-to-S conversions. These converted waves, particularly PSPP, PPSP, and PSSP modes, often re-enter the surrounding sediment as P-waves and arrive with delayed travel times. Their presence distorts structural imaging, reduces interpretability, and frequently obscures sub-salt prospectivity. Although such converted modes may occasionally enhance illumination due to wider angular coverage, their energy is more commonly treated as coherent noise that must be suppressed to improve seismic image clarity.

Converted wavefields of interest include PSPP (P-wave down, S-wave through salt, P-wave up), PPSP (P-wave down and S-wave return), and PSSP (S-wave on both down-going and up-coming paths). Among these, the symmetrical mode PSSP typically exhibits significantly longer arrival times and weaker amplitudes, due to the slower velocity of S-waves and reduced velocity contrast between

S-wave salt and surrounding P-wave sediments. In practice, PSSP is often not visible in field data, and modeling it may be unnecessary.

Conventional approaches for suppressing converted modes include filtering based on normal move-out (NMO) velocity, leveraging the slower apparent velocity of converted waves due to their S-wave component (Ogilvie and Purnell, 1996), and targeted muting of energy using travel-time ray tracing (Lu et al., 2003). However, the effectiveness of these techniques can be substantially limited when dealing with complex salt geometries. dual-leg 3D acoustic modeling has been proposed as a means to simulate converted wave energy (Huang et al., 2013), enabling its attenuation from either pre-migration or post-migration datasets. However, in areas with complex salt geometry, diffractions from the top salt can interfere with converted energy originating from the base salt, complicating forward modeling and hindering effective subtraction prior to migration. In this study, we mitigate this issue by performing two separate 3D acoustic modeling runs: one with and one without the base salt interface included in the velocity model (Kumar et al., 2018). The difference between these simulations yields a significantly cleaner representation of the converted wavefield, allowing for more effective subtraction from both pre-stack and pre-migration gathers.

To guide the selection of which converted modes to model, we utilize the diagnostic ratio r defined as the time thickness of the salt layer Δt_{salt} divided by the time difference Δt_{cw} between the primary P-wave and the converted mode base salt arrival on migrated seismic data. Under zero-offset assumptions, this ratio is expressed as:

$$r = 2 \cdot (Vs/(Vp - Vs)) \quad (1) \quad \&$$

$$r = Vs/(Vp - Vs) \quad (2)$$

The ratio for asymmetrical mode can be calculated using eq (1) and its value is generally between 2 and 3, whereas the ratio for symmetrical mode can be calculated using eq (2). The value of the ratios in this case is significantly lower, between 1 and 1.5. In the dataset analyzed in this study, the ratio was approximately 2.2, suggesting that PSPP and PPSP are the principal contributors. This information aids the selection of the type of converted mode required during the forward modelling process.

The suppression workflow begins by building a suitable P-wave interval velocity model, with careful attention to salt geometry. This model serves as the foundation for subsequent wavefield modeling. A secondary model is then constructed to include shear wave velocity within the salt, derived by scanning for the S-wave velocity that flattens observed converted mode events at the interpreted base of salt. With both models defined, we perform two sets of 3D finite-difference acoustic simulations. The first simulation includes both top and base salt interfaces and captures all relevant wavefields, including converted energy and top-salt diffractions. The second simulation omits the base salt reflectors, modeling only wave propagation through the top salt. By subtracting the results of the second simulation from the first, we obtain a clean converted wave model containing only the desired PSPP and PPSP modes. This differential approach minimizes contamination by top-salt diffractions and isolates converted energy originating from the base salt.

The resulting converted wave model is then adaptively subtracted from the field data. Subtraction is performed using an intelligent method that combines least-squares filtering in the time-space domain with curvelet-domain subtraction techniques. This hybrid approach compensates for mismatches in amplitude and timing caused by velocity model inaccuracies or interpretation uncertainties. Moreover, it preserves primary energy by treating the converted model as a 'true noise model' ensuring that only the modeled converted wave energy is removed. This process is especially important in complex salt environments, where converted waves overlap with key reflection events.

The converted mode model obtained from the first forward modeling step can be directly used for suppression; however, this approach requires subtraction in the image domain, where top-salt diffractions have collapsed and no longer obscure the converted energy. In contrast, performing an additional modeling run and computing the difference between the two simulations enables a cleaner separation of the converted wavefield, facilitating more effective suppression in the data domain.

The method delivers reliable converted energy attenuation while preserving the seismic primaries critical for interpretation. It is particularly effective in geologically complex settings, making it well suited for exploration scenarios where sub-salt illumination is vital.

Example

The seismic data example was acquired as part of a multi-client campaign in the Eastern Mediterranean Sea, offshore Egypt, with water depths ranging from 200 m to 3000 m. The campaign covered area over many blocks as shown in Figure 3. A very similar processing sequence was applied to those blocks and subsequently the data from all blocks were merged to produce a seamless mega volume of approximately 35000 sqkm. The proposed flow has been applied where the converted mode energy is obvious which typically occurs at thick salt sections.

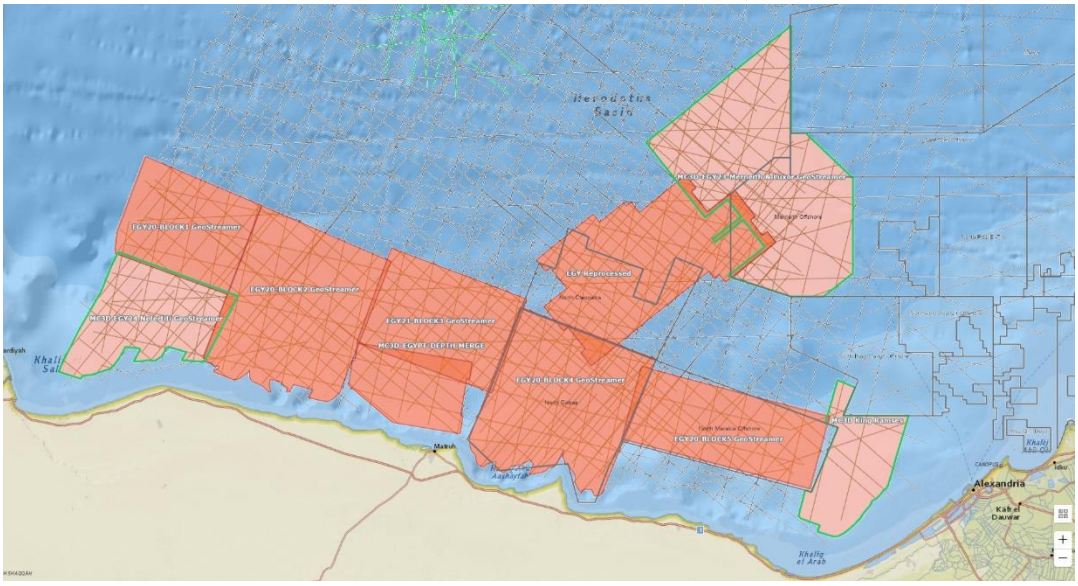

Figure 1: Different blocks acquired in the multi-client campaign in the Eastern Mediterranean Sea, offshore Egypt.

The modelling of symmetrical modes (PSSP) was ignored in the below cases, owing to a lack of evidence of its presence in the recorded field data. The ratio (r), described in equations (1) and (2), was estimated at 2.2, inferring that the converted mode was recorded with only one of the up-coming or down-going wave-fields as an S-wave in the salt layer; either PSPP, or PPSP, or both.

Case study 1

This survey was acquired in Block1 using a triple-source configuration and twelve 10 km long multisensor streamers at a depth of 20 m separated by 150 m. The nominal seismic acquisition bin size was 6.25 m by 25 m, with 100-fold coverage. The size of the survey is 2695 km^2 and the water depth between 2000m to 3000m.

The velocity model for the modelling was generated using tomography in the post-salt section to estimate the sediment velocity. The salt layer velocity was estimated using a salt flooding methodology after interpreting the top salt reflection. The aim of this flooding step was to estimate the P-wave velocity that produces optimal flatness of the base salt reflection. S-wave velocity was obtained by scanning for the velocity which flattens the converted mode energy at the same depth as the interpreted base salt. For this dataset, the P-wave velocity of the salt was estimated at 4200 m/s, whereas the Swave velocity was estimated at 2200 m/s. FWI was used in the velocity model building workflow, but it was not included in the velocity model for converted waves modelling.

Figure 2 shows the shot gathers with and without the proposed converted wave attenuation flow. The arrow shows the location in shot gather where the converted wave was recorded in data domain. Figure 2 clearly shows effective attenuation of the recorded converted wave.

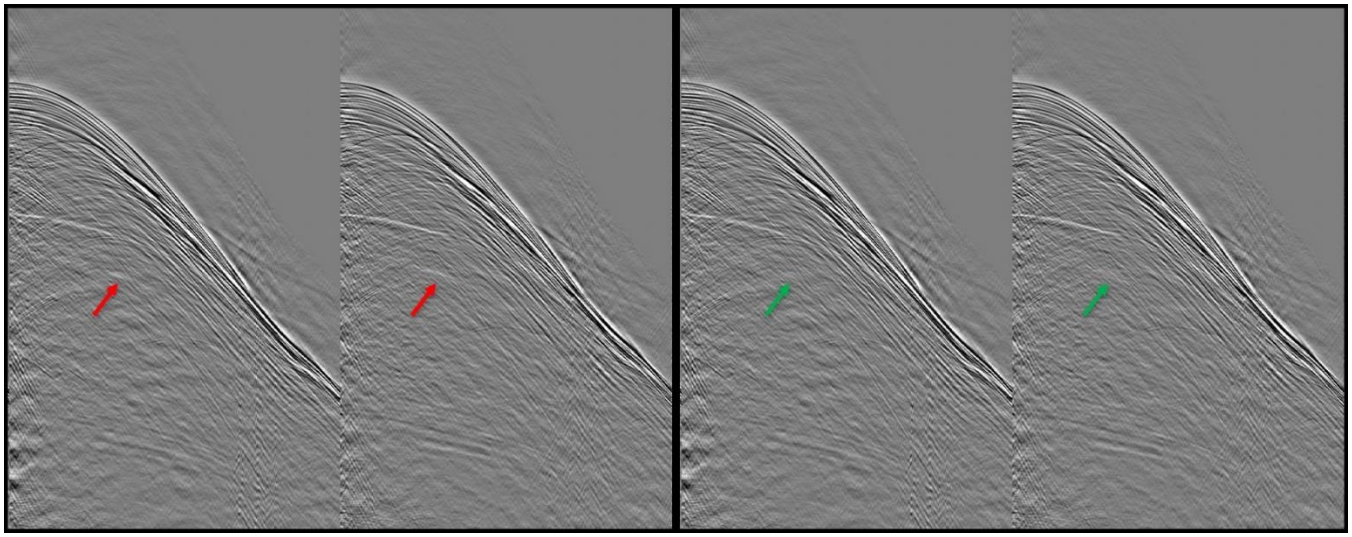

Figure 2: Shot gathers without converted wave attenuation flow left and with converted wave attenuation flow right

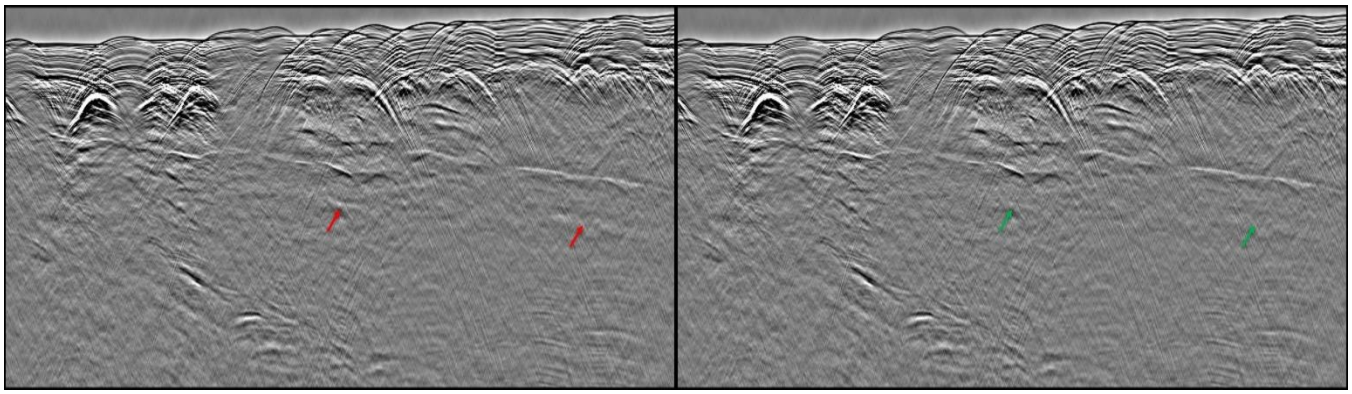

Figure 3: Stack in the data domain without converted wave attenuation flow left and with converted wave attenuation flow right

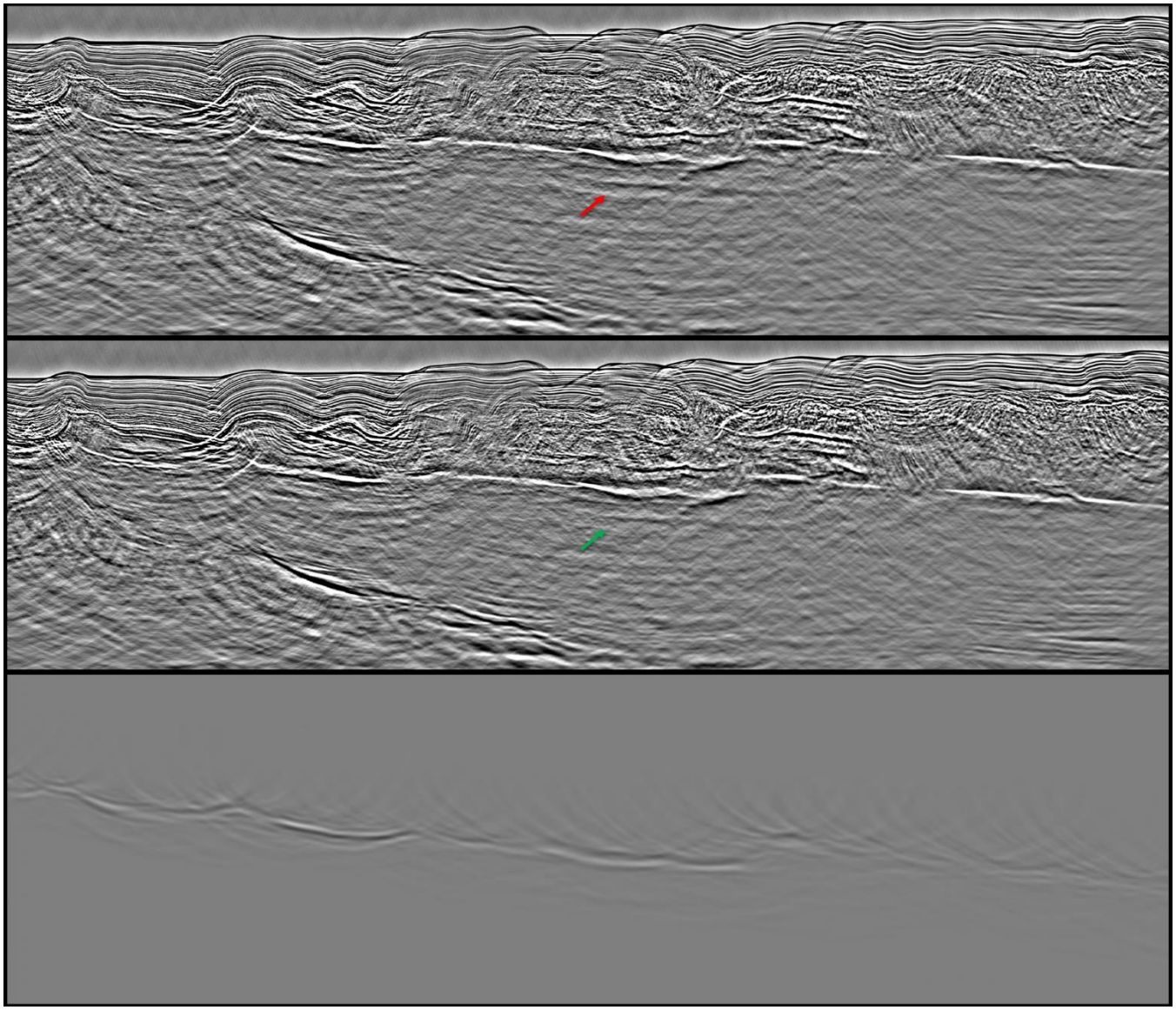

Figure 4: Image domain stack obtained by migrating data using Kirchhoff algorithm without converted wave attenuation flow top and with converted wave attenuation flow middle and the difference display bottom.

While it is harder to observe the converted wave on shot gathers, Figure 3 shows that the converted waver energy can be easily identified in the pre-migration stack. Examining both the top and base of the salt in the stack reveals the complexity of the salt layer, which adds further challenges to accurately modeling and subtracting the converted wave energy. The arrows highlight the locations of the recorded converted wave energy on the pre-migration stack section. It is evident that the proposed workflow has effectively attenuated the converted wave energy. The image domain QC, on migrated stack obtained using Kirchhoff algorithm, is shown in figure 4, highlighting the effective attenuation of the converted wave in such complex salt regime. The difference display shows nice isolation of the converted wave event.

Case study 2

This example is from Block3, the total area acquired is 3136 km^2. The survey was acquired with a configuration using 12 dual-sensor streamers, each 10000-m long, three source arrays were used shooting at an interval of 16.667 m. The nominal seismic acquisition bin size was 6.25 m by 25 m.

Similar velocity model has been generated as in case study 1 where tomography is used in the post-salt section to estimate the sediment velocity, and the salt layer velocity was estimated using a salt flooding methodology after interpreting the top salt reflection. Base salt

interpretation was performed to constrain the salt layer using appropriate salt velocity obtained from salt flood methodology.

Figure 5 & 6 shows a common shot gather and stack in data domain from the survey area annotated with the location of the asymmetrical mode converted energy, and results after the mode converted energy has been removed. The effectiveness of the converted energy removal is clearly visible in the data domain. Figure 7 shows Kirchhoff depth stack images before and after the removal of the mode converted energy. The absence of the converted wave in the middle of the migrated stack is attributed to the salt benching out, resulting in no interface for mode conversion.

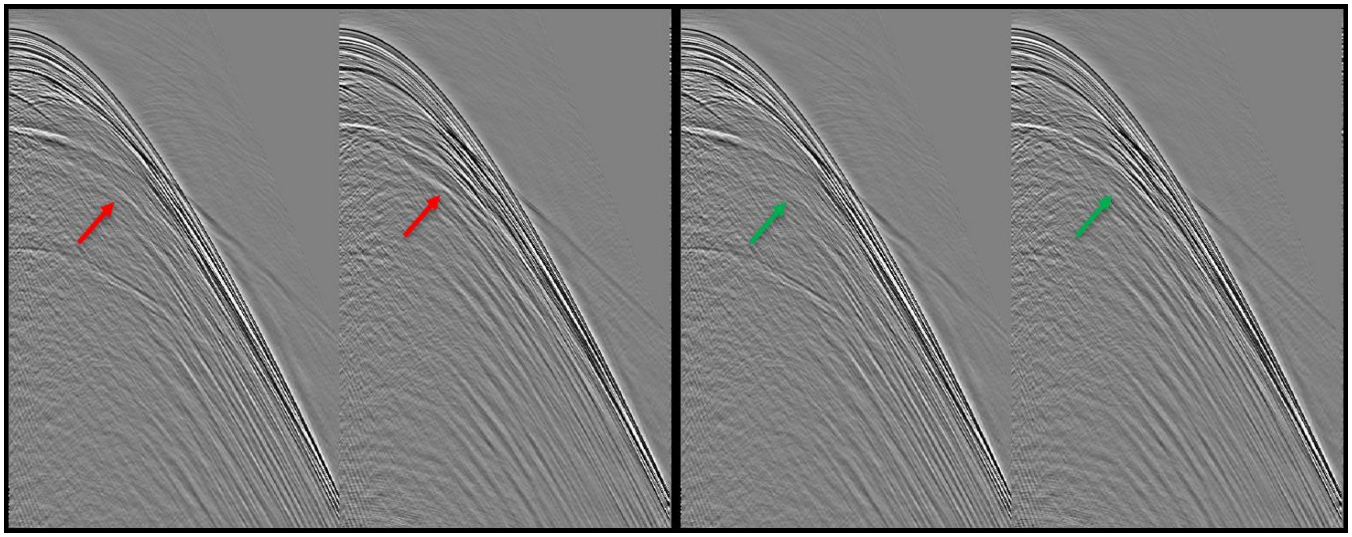

Figure 5: Shot gathers without converted wave attenuation flow left and with converted wave attenuation flow right

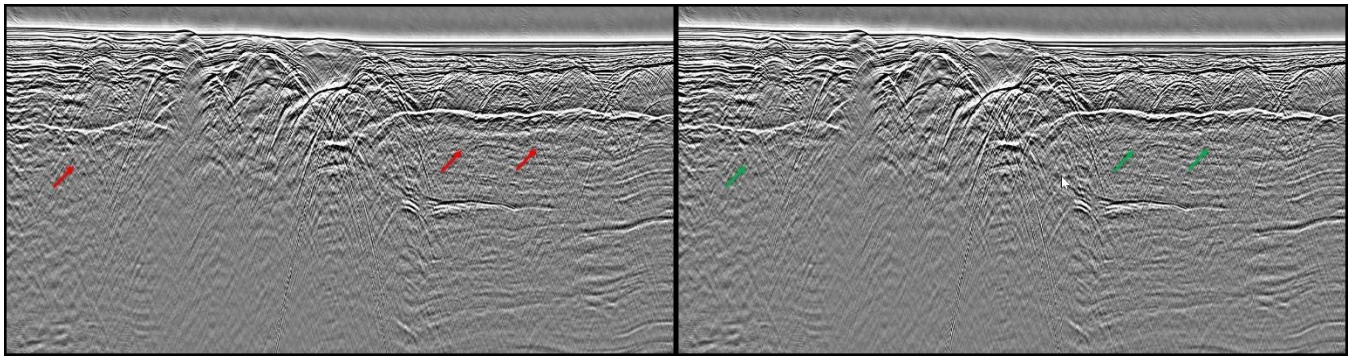

Figure 6: Stack in the data domain without converted wave attenuation flow left and with converted wave attenuation flow right

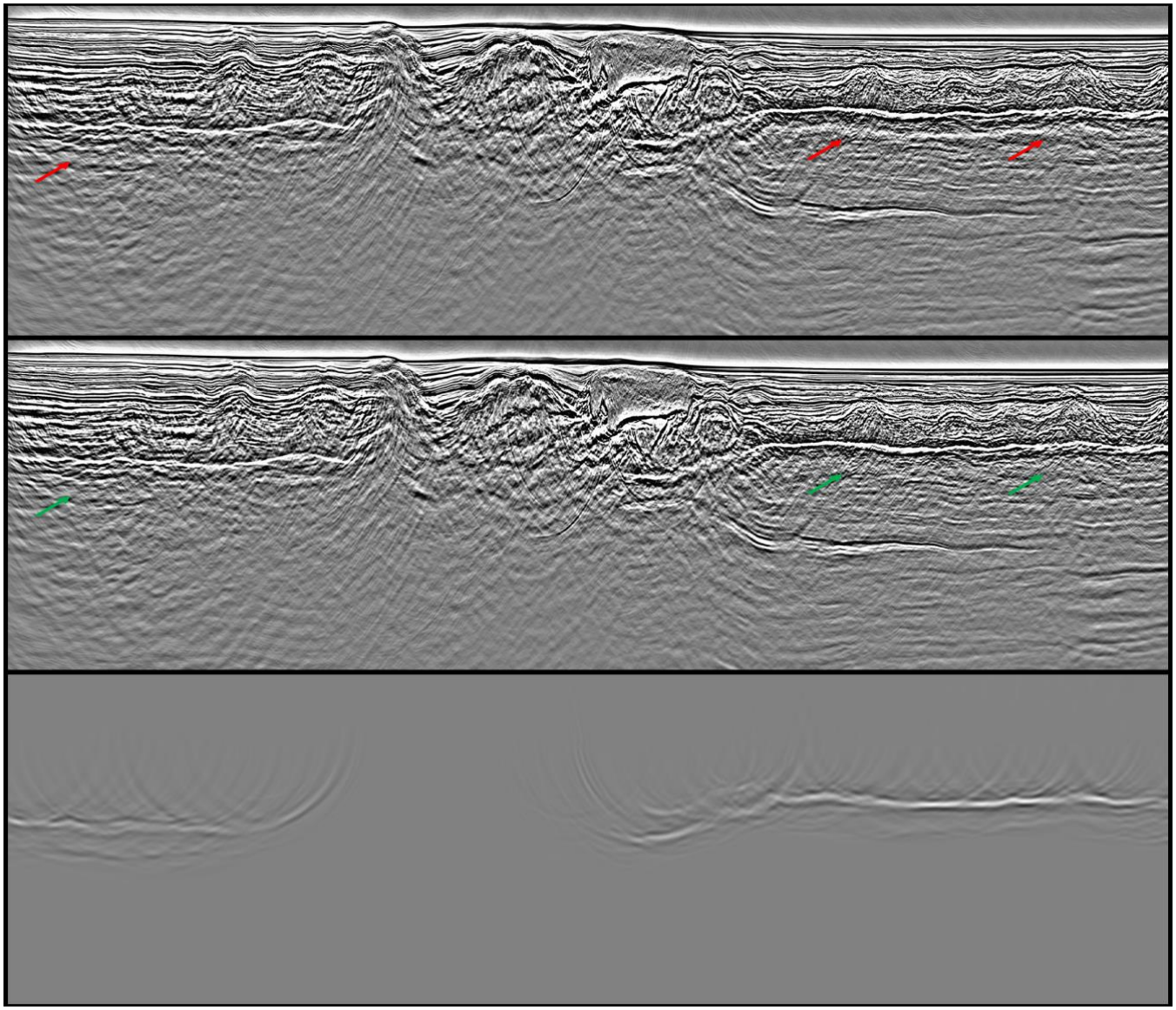

Figure 7: Image domain stack obtained by migrating data using Kirchhoff algorithm without converted wave attenuation flow top and with converted wave attenuation flow middle and the difference display bottom.

Case study 3

This example is from Merneith & Luxor, the total area acquired is 6715 km^2. The acquisition parameters are very similar to the previous survey with a triple-source configuration and twelve 10 km long multisensor streamers at a depth of 20 m separated by 150 m. The nominal seismic acquisition bin size was 6.25 m by 25 m, with 100-fold of coverage.

The velocity model used for the converted wave modeling was derived through tomography focused on the post-salt section to estimate sediment velocities. During the salt body velocity analysis, certain areas were identified as containing dirty salt, which required a lower average velocity compared to regions of clean salt. A spatially varying salt velocity was implemented, using a background clean salt velocity of 4400 m/s, while assigning slower velocities in the dirty salt regions to optimize gather flatness at the base of the salt.

Within this large exploration area, the composition of Messinian salt varied significantly from thick, pure salt in the northwest to a more contaminated, mixed salt in the southeast. This variation had a notable impact on the observable converted wave in the dataset. In areas with cleaner salt, the converted wave appeared stronger and more continuous, whereas in regions with dirty salt, the converted wave energy weakened and became less visible in seismic data.

To explore the link between converted wave (CW) coherency and salt purity, Figure 8 presents a comparison between a converted wave amplitude (CWA) map and a salt dirtiness map. The CW coherency map was generated by calculating the RMS amplitude within a ±100 ms window around the expected CW time. For the salt dirtiness map, the RMS amplitude was calculated from 100 ms below the

top salt boundary to 100 ms above the base salt. A stronger amplitude within the salt layer indicates more dirtiness within Messinian salt. As shown in Figure 1a, the converted wave is stronger and more continuous in the western areas, which correspond to regions of cleaner salt in Figure 1b. In contrast, Figure 1b exhibits higher salt dirtiness in the eastern regions, corresponding to the presence of weaker converted waves in Figure 1a.

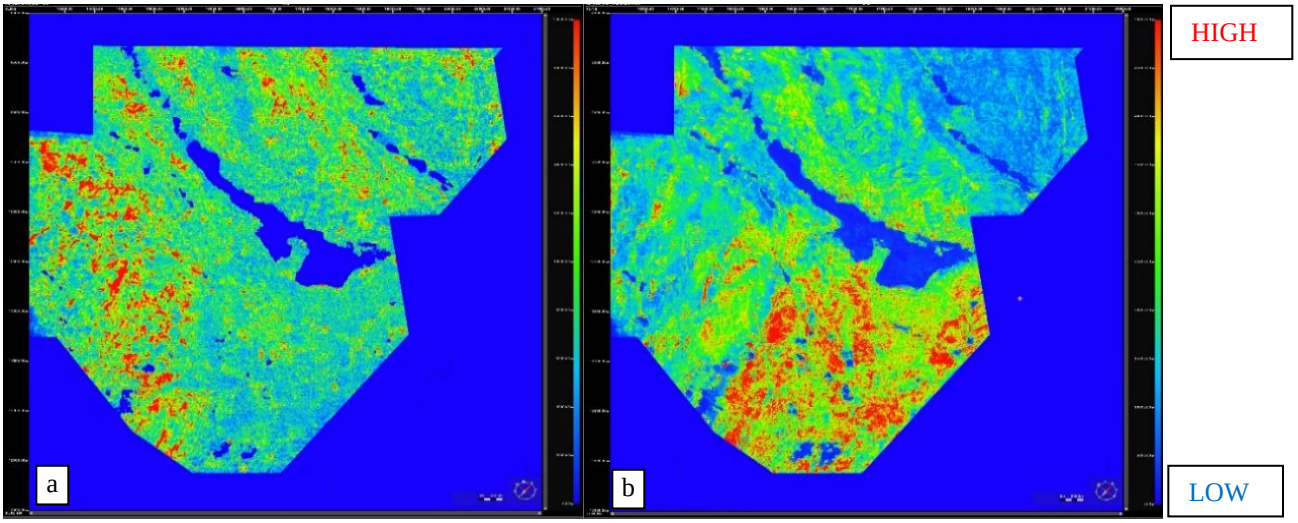

Figure 8: The converted wave coherency map (a) the salt dirtiness map (b)

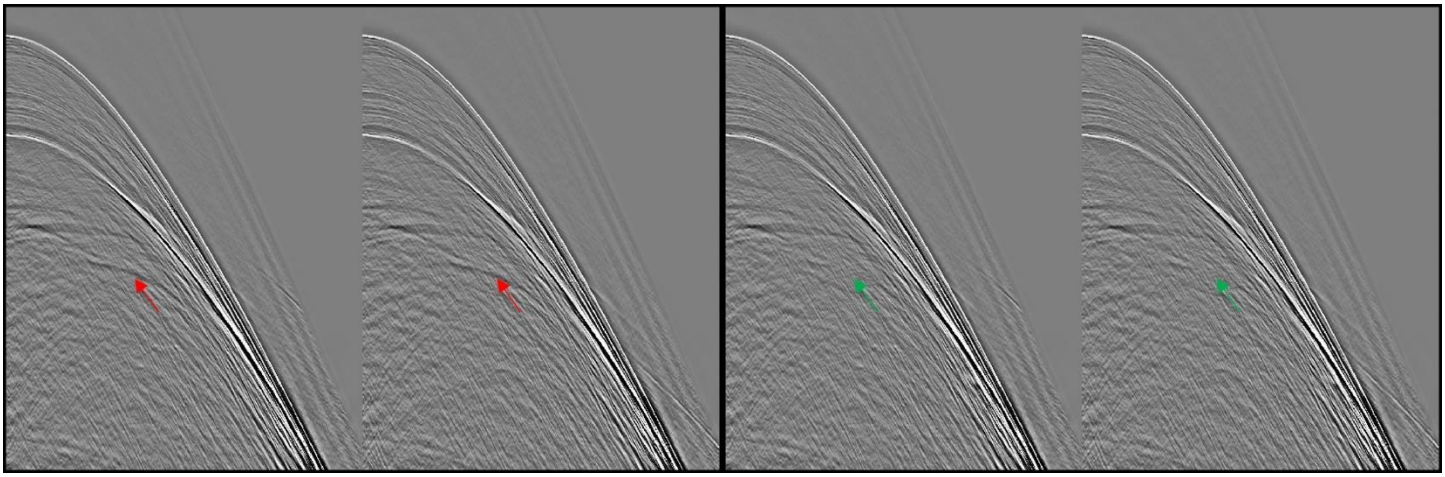

Figure 9: Shot gathers without converted wave attenuation flow left and with converted wave attenuation flow right

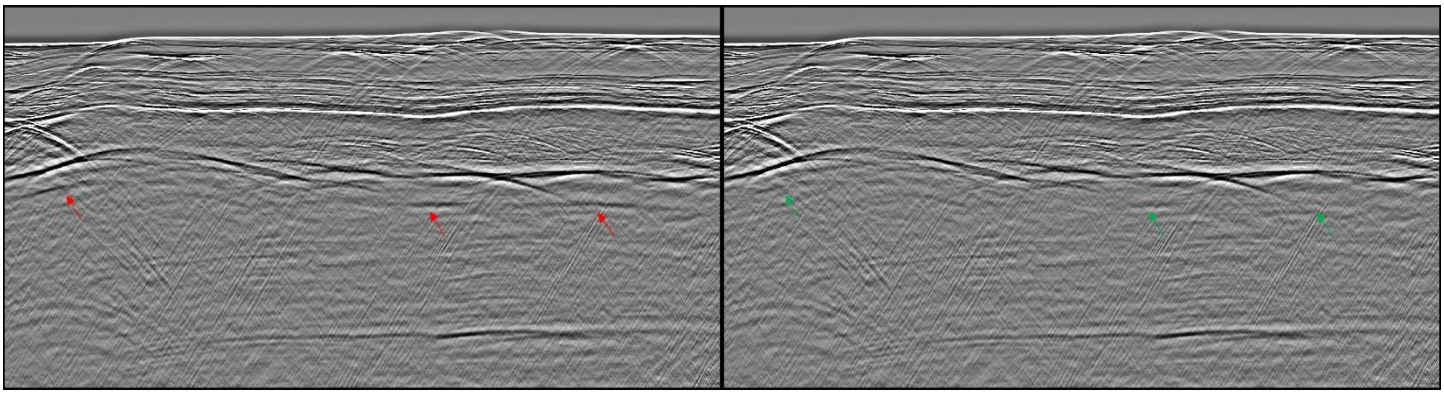

Figure 10: Stack in the data domain without converted wave attenuation flow left and with converted wave attenuation flow right

The effective application of the converted wave attenuation flow is clearly visible on the shot and stack display in figures 9 and 10. The arrows in the figure indicate the location of the recorded converted wave, which is clearly significantly attenuated using the proposed workflow.

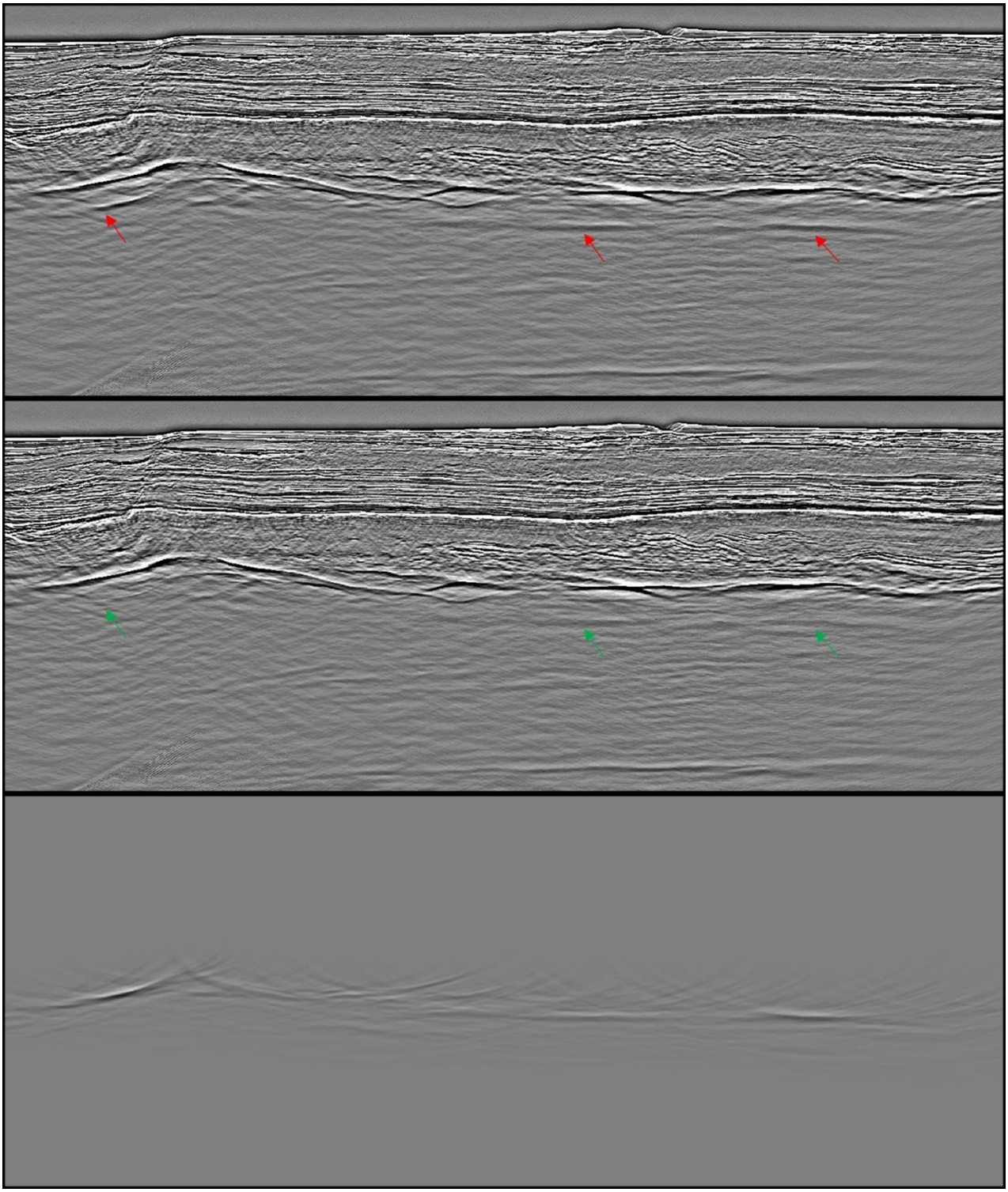

Figure 8: Image domain stack obtained by migrating data using Kirchhoff algorithm without converted wave attenuation flow top and with converted wave attenuation flow middle and the difference display bottom.

Figure 10 shows the result in the image domain obtained by migrating data using Kirchhoff algorithm. In image domain, the converted wave shows different levels of amplitude strength along the line due to the complexity of the salt in this region, but the converted wave was successfully modelled and subtracted from the input data as shown in Figure 10.

Conclusion

Sub-salt prospects in the Mediterranean are often challenged by complex salt geometries and the presence of converted wave energy. Our study, conducted in three separate locations with variable salt complexity, demonstrates that a straightforward yet robust attenuation workflow can effectively suppress both asymmetrical (PSPP, PPSP) or symmetrical (PSSP) converted modes. This enhances pre-salt reflectivity, improves data interpretability, and reduces exploration risk.

Acknowledgement

The authors would like to thank TGS MultiClient for granting permission to present examples from various surveys conducted by TGS across the Mediterranean Sea. Special appreciation goes to the TGS geophysicists whose support was instrumental in generating the results.

References

Elbassiony, A., Kumar, J. and Martin, T. [2018]. Velocity model building in the major basins of the eastern Mediterranean Sea for imaging regional prospectivity. The Leading Edge, 37(7), 519-528

Huang, Y., W. Gou, O. Leblanc, S. Ji, and Y. Huang, 2013, Salt-related converted-wave modeling and imaging study: 75th Annual EAGE Conference and Exhibition, Tu 01 13.

Jones, I. F., and I. Davison, 2014, Seismic imaging in and around salt bodies: Interpretation, 2, 4, SL1–SL20.

Kumar, J., Bell, M., Salem, M., Martin, T. and Fairhead, S. [2018]. Mode conversion noise attenuation, modelling and removal: case studies from Cyprus and Egypt. First Break, 36, 113–120.

Lu, R. S., D. E. Willen, and I. A. Watson, 2003, Identifying, removing and imaging P-S-conversions at salt-sediment interfaces: Geophysics, 68, 3, 1052–1059.

Ogilvie, J. S., and G. W. Purnell, 1996, Effects of salt-related mode conversions on subsalt prospecting: Geophysics, 61, 2, 331–348

Perrier, S., Dyer, R., Liu, Y., Nguyen T. and Lecocq, P. [2017]. Intelligent adaptive subtraction for multiple attenuation. 79th Annual EAGE Conference and Exhibition, We B3 03